Molecular Biology of the Cell
Vol. 12, 239–250, January 2001

Mutant Caldesmon Lacking cdc2 Phosphorylation Sites Delays M-Phase Entry and Inhibits Cytokinesis

Shigeko Yamashiro, Hueylan Chern, Yoshihiko Yamakita, and Fumio Matsumura

Department of Molecular Biology and Biochemistry, Rutgers University, Nelson Labs, Busch Campus, Piscataway, New Jersey 08855

Submitted April 20, 2000; Revised September 7, 2000; Accepted October 23, 2000
Monitoring Editor: Thomas D. Pollard

Caldesmon is phosphorylated by cdc2 kinase during mitosis, resulting in the dissociation of caldesmon from microfilaments. To understand the physiological significance of phosphorylation, we generated a caldesmon mutant replacing all seven cdc2 phosphorylation sites with Ala, and examined effects of expression of the caldesmon mutant on M-phase progression. We found that microinjection of mutant caldesmon effectively blocked early cell division of *Xenopus* embryos. Similar, though less effective, inhibition of cytokinesis was observed with Chinese hamster ovary (CHO) cells microinjected with 7th mutant. When mutant caldesmon was introduced into CHO cells either by protein microinjection or by inducible expression, delay of M-phase entry was observed. Finally, we found that 7th mutant inhibited the disassembly of microfilaments during mitosis. Wild-type caldesmon, on the other hand, was much less potent in producing these three effects. Because mutant caldesmon did not inhibit cyclin B/cdc2 kinase activity, our results suggest that alterations in microfilament assembly caused by caldesmon phosphorylation are important for M-phase progression.

INTRODUCTION

Microfilaments undergo profound changes in their cytoplasmic organization during mitosis of cultured cells. When cells enter prophase, stress fibers are disassembled concomitant with cell rounding. During cytokinesis, microfilaments transiently form contractile rings for cytoplasmic division. After cytokinesis, microfilaments reassemble into stress fibers of the two daughter cells as the cells spread on substrates.

We have previously shown that nonmuscle caldesmon is dissociated from microfilaments during mitosis, apparently as a consequence of mitosis-specific phosphorylation (Yamashiro *et al.*, 1990). Subsequently, we, as well as others, demonstrated that cdc2 kinase, a catalytic subunit of maturation- or mitosis-promoting factor, phosphorylates caldesmon from nonmuscle and smooth muscle sources (Mak *et al.*, 1991; Yamashiro *et al.*, 1991). These findings suggest that maturation- or mitosis-promoting factor directly regulates the microfilament reorganization during mitosis via cell cycle-dependent phosphorylation of caldesmon.

Caldesmon is an actin- and calmodulin-binding protein, whose actin binding is regulated by Ca^{2+}/calmodulin (reviewed by Sobue *et al.*, 1981; Matsumura and Yamashiro, 1993; Huber, 1997). In addition to binding F-actin and calmodulin, caldesmon is known to bind to other proteins, including tropomyosin and myosin. In an in vitro reconstituted system, caldesmon inhibits actomyosin ATPase activity. In vivo studies using smooth muscle cells have supported the inhibitory function of caldesmon in smooth muscle contraction (Katsuyama *et al.*, 1992; Pfitzer *et al.*, 1993; Huber, 1997; Earley *et al.*, 1998; Burton and Marston, 1999). A recent report has implied a similar function for caldesmon in nonmuscle cells (Helfman *et al.*, 1999).

There is a body of evidence indicating that caldesmon stabilizes microfilaments in nonmuscle cells (reviewed by Matsumura and Yamashiro, 1993; Huber, 1997). In vitro, caldesmon enhances actin/tropomyosin binding (Bretscher, 1984; Yamashiro-Matsumura and Matsumura, 1988), which appears to protect actin filaments from actin-depolymerizing or -severing proteins in vitro. For example, caldesmon together with tropomyosin protects actin filaments against the actin-severing and -capping activities of gelsolin (Ishikawa *et al.*, 1989a,b). In vivo, microfilaments became more resistant to cytochalasin when the COOH-terminal actin- and calmodulin-binding domain of caldesmon was overexpressed in Chinese hamster ovary (CHO) cells (Warren *et al.*, 1994). Caldesmon also is responsible for glucocorticoid-induced stabilization of the actin cytoskeleton in A549 cells (Castellino *et al.*, 1995). Glucocorticoid treatment induced caldesmon expression, and resulted in the formation of more stress fibers in A549 cells. More importantly, a caldesmon

* Corresponding author. E-mail address: yamashiro@mbcl.rutgers.edu or matsumura@mbcl.rutgers.edu.

antisense oligodeoxynucleotide dramatically inhibited both glucocorticoid-induced caldesmon synthesis and stress fiber assembly with similar potencies. Furthermore, microinjection of an antibody against the COOH-terminal actin/calmodulin-binding domain of caldesmon resulted in the disruption of stress fibers (Lamb *et al.*, 1996).

We previously demonstrated that mitosis-specific phosphorylation of nonmuscle caldesmon by cdc2 kinase resulted in the loss of a variety of properties of caldesmon. Phosphorylated caldesmon exhibited much reduced binding to actin, calmodulin, and myosin, and phosphorylated caldesmon was not able to inhibit actomyosin ATPase activity (Yamashiro *et al.*, 1990, 1991; Yamakita *et al.*, 1992). We identified seven cdc2 phosphorylation sites, all of which were located in the COOH-terminal half of the molecule (Yamashiro *et al.*, 1995). Because the COOH terminus is responsible for actin and calmodulin binding, as well as the inhibition of actomyosin ATPase of caldesmon, we generated a mutant of the COOH terminus replacing all seven sites with alanine, and analyzed the effects of cdc2 phosphorylation on its actin- and calmodulin-binding activities, as well as its ability to inhibit actomyosin ATPase. We found that the mutant COOH terminus was not phosphorylated by cdc2 kinase and thus did not show any changes in its properties after treatment with cdc2 kinase. On the other hand, a wild-type counterpart was phosphorylated effectively by cdc2 kinase and its properties were greatly inhibited (Yamashiro *et al.*, 1995). These results indicate that phosphorylation of these seven sites by cdc2 kinase regulates caldesmon's actin and calmodulin binding, as well as the inhibition of actomyosin ATPase.

We hypothesized that phosphorylation-dependent alterations in the properties of caldesmon are involved in the microfilament reorganization observed during mitosis. To elucidate the physiological function of mitosis-specific phosphorylation of caldesmon during mitosis, we generated a mutant of the whole molecule of caldesmon in which all seven cdc2 phosphorylation sites were replaced with alanine (called 7th mutant). Such a mutant would stay bound to microfilaments during mitosis and could affect M-phase progression. We found that the expression of the mutant stabilized the microfilament cytoskeleton, delayed entry into M-phase, and inhibited cell division.

MATERIALS AND METHODS

Plasmid Preparation

Using a cDNA clone (called D3 clone) encoding the COOH-terminal half of rat nonmuscle caldesmon, we previously generated a mutant of D3, in which all seven Ser or Thr phosphorylation sites of cdc2 kinase were replaced with Ala (Yamashiro *et al.*, 1995). The nonmutated and mutated D3 cDNA clones were subcloned into a pBluescript SK(−) vector (Stratagene, La Jolla, CA), and another caldesmon cDNA clone (called A16), which encoded the NH_2-terminal half of caldesmon, was inserted to generate full-length wild-type and mutant (7th mutant) caldesmon cDNAs. These two full-length clones were myc-tagged by polymerase chain reaction, and subcloned into the *Nco*I and *Bam*HI sites of a bacterial expression vector, pET 11d (Novagen, Madison, WI), and used for the bacterial expression of wild-type and 7th mutant caldesmon as described below.

Purification of Wild-Type and Mutant Caldesmon

The expression of caldesmon was induced by the addition of 0.4 mM isopropyl β-D-thiogalactoside. After induction, bacteria were incubated for 2–3 h at 25°C to minimize degradation of caldesmon. The purification of wild-type and 7th caldesmon was performed as described previously (Yamashiro-Matsumura and Matsumura, 1988). Briefly, the bacteria were homogenized using French Press apparatus in 20 mM Tris-HCl of pH 8.0 containing 0.1 M NaCl, 1 mM dithiothreitol (DTT), 1 mM EDTA, and protease inhibitors (1 mM phenylmethylsulfonyl fluoride, 1 mM benzamidine, 10 μg/ml leupeptin, 10 μg/ml aprotinin). After centrifugation at 10,000 rpm for 10 min, the supernatant was heat-treated at 95°C for 10 min, cooled on ice for 30 min, and centrifuged again. The supernatant was fractionated by ammonium sulfate between 0 and 28 g/100 ml of the supernatant. After dialysis, the ammonium sulfate fraction was applied on a DEAE cellulose column (equilibrated with 20 mM Tris-HCl of pH 8.0, 0.5 mM DTT, 0.2 mM phenylmethylsulfonyl fluoride, 0.1 mM EDTA), and eluted by a gradient from 0 to 0.5 M NaCl. Caldesmon-containing fractions were finally purified on a calmodulin-Sepharose column. The purified fractions were concentrated using Centricon 30 (Amicon, Beverly, MA) to a final concentration of 5–10 mg/ml.

Microinjection into Xenopus *Eggs*

Wild-type and 7th mutant caldesmon were dialyzed against *Xenopus* microinjection buffer (88 mM NaCl, 10 mM HEPES, pH 6.8). Eggs from *X. laevis* were fertilized in vitro and cultured in 0.3× MMR (33 mM NaCl, 0.67 mM KCl, 0.33 mM $MgCl_2$, 0.67 mM $CaCl_2$, 0.033 mM EDTA, 1.67 mM HEPES, pH 7.8) containing 5% Ficol 400. The embryos were selected at the beginning of the first furrow, which was ~90 min after fertilization. Either 25 or 50 nl of caldesmon samples (10 mg/ml) was injected into one blastomere of embryos at the two-cell stage.

Microinjection into CHO Cells Synchronized for Cell Division

Microinjection was performed as described (Yamakita *et al.*, 1990). Wild-type or mutant caldesmon (5 mg/ml) was dialyzed against injection buffer containing 10 mM sodium phosphate buffer of pH 7.2 containing 77 mM KCl, and injected into CHO cells. Synchronization of CHO cells was performed as follows. CHO cells grown in F12 medium containing 10% fetal calf serum were treated with 4 mM thymidine for 15 h to arrest cells at the beginning of S phase. After washing out thymidine, cells were incubated for 4 h to allow S-phase progression, and then treated for 3–4 h with 0.25 μg/ml nocodazole to arrest at the prometaphase. Approximately 35–45% of cells were arrested at mitosis in this way.

Transfection

The myc-tagged, full-length wild-type and 7th mutant caldesmon cDNAs were subcloned into the *Not*I and *Xba*I sites of a pIND vector, an ecdysone-inducible expression vector (Invitrogen, Carlsbad, CA), and transfected into EcR-CHO cells that stably expressed the ecdysone receptor from a pVgRXR vector (Invitrogen). After selection by G418 treatment for 2 wk, clones were isolated, and examined for inducible expression of wild-type or 7th mutant caldesmon by immunofluorescence as follows: Cells on a coverslip were treated with 3 μM muristerone A for 24 h, and stained with an antibody against the myc tag. Positive clones were selected and propagated to examine effects of caldesmon expression on cell cycle progression.

Immunofluorescence and Image Processing

Immunofluorescence was performed using formaldehyde fixation as described (Yamashiro *et al.*, 1998). Exogenously expressed wild-

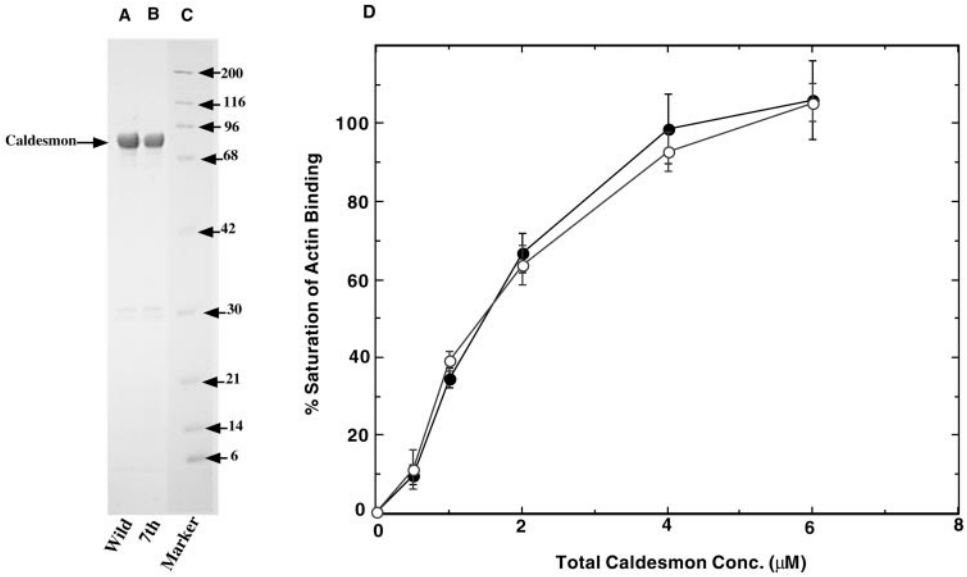

Figure 1. SDS-PAGE of bacterially expressed, purified wild-type, and mutant rat caldesmon. Both wild-type and mutant caldesmon were expressed in bacteria, and purified by DEAE-cellulose followed by calmodulin-Sepharose column. Both wild-type and mutant caldesmon showed >95% purity. Lane A, wild-type caldesmon; lane B, 7th mutant caldesmon; lane C, molecular mass markers (indicated in kDa at the right of the figure). (D) Actin binding of wild-type and 7th mutant caldesmon. ○, wild-type caldesmon; ●, 7th mutant caldesmon.

type and mutant caldesmon were detected by immunofluorescence by using anti-myc monoclonal antibody (9E1). F-actin was visualized using fluorescently labeled phalloidin (Sigma, St. Louis, MO). Phase and fluorescence images were taken with a Nikon TE300 inverted microscope equipped with an AT200 Photometrics cooled charge-coupled device camera (Roper Scientific Inc, Tucson, AZ). Some images were deconvolved using MicroTome image processing software (VayTek, Fairfield, IA).

Fluorescent intensities of caldesmon and F-actin were quantified as follows. Mock-transfected, wild-type caldesmon-expressing, and 7th mutant caldesmon-expressing cells were double labeled with the myc antibody and fluorescent phalloidin precisely in the same way. Pairs of myc and phalloidin staining images were taken with the AT200 charge-coupled device camera under the same conditions, and any images showing intensity saturation were excluded from analysis. Background fluorescence was obtained from a cell-free field of each image and subtracted. Cells expressing exogenous caldesmon were randomly selected from each pair of images, and mean fluorescent intensities (to compensate differences in a cell size) of both myc and phalloidin staining were quantified using the public domain NIH image program (http://rsb.info.nih.gov/nih-image/). More than 70 cells were examined and three independent experiments were performed.

Immunoprecipitation and Kinase Assay

Cyclin B/cdc2 complexes were immunoprecipitated from mitotically arrested HeLa cells. Mitotically arrested HeLa cells prepared as described previously (Yamakita *et al.*, 1992) were lysed with immunoprecipitation buffer (30 mM Tris-HCl, pH 7.5, 150 mM KCl, 25 mM $Na_4P_2O_7$, 1 mM Na_3VO_4, and 1% Triton X-100). Cell lysates were incubated with anti-cyclin B1 antibody (Biosource International, Camarillo, CA), and the immune-complexes were precipitated with Protein G Sepharose (Amersham Pharmacia, Piscataway, NJ). After extensive washing with the immunoprecipitation buffer, the immune-complexes were washed with kinase buffer (50 mM Tris-HCl, pH 7.5, 10 mM $MgCl_2$, 50 mM NaCl, 1 mM EGTA, 2 mM DTT). Kinase reactions were performed at 30°C for 10 min in the kinase buffer containing 100 μM ATP (50 μCi [γ-^{32}P]ATP/ml), 500 nM peptide inhibitor to A-kinase (Sigma) and 0.25 μM histone H1 (Boehringer-Mannheim, Indianapolis, IN) with or without wild-type or mutant caldesmon (1.2 μM). The reactions were stopped by the addition of 2× SDS sample buffer, and the samples were analyzed by SDS-PAGE. Histone H1 kinase activities of cyclin B/cdc2 immune-complexes were quantitated by a PhosphorImager (Amersham Pharmacia). The effects of caldesmon also were examined using recombinant cdc2 kinase (New England Biolabs, Beverly, MA).

Other Procedures

Actin binding of purified wild-type and mutant caldesmon was assayed as described previously (Yamashiro-Matsumura *et al.*, 1988). Protein concentrations were determined by the method of Bradford (1976) by using bovine serum albumin as standard.

RESULTS

Purification and Characterization of Caldesmon Mutant

We expressed, in bacteria, full-length rat nonmuscle caldesmon, as well as its mutant in which all seven cdc2 phosphorylation sites were mutated to Ala (called 7th mutant). Figure 1 shows an SDS-PAGE pattern of purified wild-type caldesmon and 7th mutant, indicating that both proteins are >95% pure. We examined actin-binding abilities of both wild-type caldesmon and 7th mutant and confirmed that both proteins showed indistinguishable actin binding (Figure 1D). When these caldesmons were phosphorylated with cdc2 kinase, only wild-type, but not mutant, caldesmon showed greatly decreased actin binding (our unpublished results). These results would be expected from our previous reports that cdc2 phosphorylation of caldesmon greatly decreases its actin-binding ability (Yamashiro *et al.*, 1990, 1991; Yamakita *et al.*, 1992). They are consistent with our previous results with the mutant of the COOH terminus of rat nonmuscle caldesmon in which all seven cdc2 phosphorylation sites were replaced with Ala (Yamashiro *et al.*, 1995).

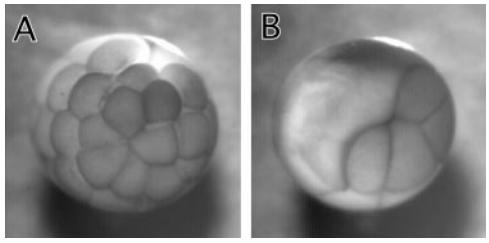

Figure 2. Block of cell division of *Xenopus* embryos by microinjection of 7th mutant. Wild-type or 7th mutant caldesmon was injected into one blastomere at two-cell stage of *Xenopus* embryos. (A) Injection with wild-type caldesmon. (B) Injection with 7th mutant caldesmon.

Blockage of Cell Division of Xenopus *Embryo by Microinjection of the Mutant Caldesmon*

We first examined the effect of 7th mutant on cell division of *Xenopus* embryos. Because the cell division of *Xenopus* embryos is well synchronized and rapid (~30-min intervals), the system is suitable for examining the mutant's effects. We microinjected into one of two blastomeres at the two-cell stage so that an uninjected blastomere provided an internal control to monitor cell division. As Figure 2 shows, microinjection of 50 nl of 7th mutant (10 mg/ml) blocked cell division of the injected blastomere, whereas the uninjected blastomere underwent multiple cell divisions (Figure 2B). On the other hand, the injection of the same concentration of wild-type caldesmon did not block cytokinesis in a majority of injected blastomeres (Figure 2A).

Table 1 summarizes the quantitative data on the effects of caldesmon injection. Microinjection of 50 nl of injection buffer alone had virtually no effect on cell division (n = 42). The microinjection of mutant caldesmon with the same volume, however, greatly affected cell division (n = 60): Cell division was arrested in 63% of injected embryos. The rest showed delayed cytokinesis (the interval between cell division is prolonged from normal 20–30 min to 2–4 h). In contrast, wild-type caldesmon had much less effect: 66% of embryos injected with wild-type caldesmon showed normal cell division, whereas 5 and 29% of embryos exhibited block and delay of cytokinesis (n = 64), respectively. The delay with wild-type caldesmon is 1–2 h, which is shorter than that of mutant caldesmon. The mutant still showed potent effects on cell division even when the injection volume was reduced to half (25 nl). Injection of 7th caused blockage of cell division in 14% and delay in 82% of embryos (n = 22), whereas wild type caused blockage in only 2% and delay in 37% of embryos (n = 41).

We examined the concentration of endogenous caldesmon in *Xenopus* eggs and estimated to what extent the injections into blastomeres increase the concentrations of caldesmon. We found two forms of caldesmon with apparent M_r of 90,000 (major isoform) and 170,000, the identity of which was confirmed by Western blotting as well as calmodulin and actin binding (our unpublished results). Quantitative Western blotting elucidated that *Xenopus* eggs contained ~6–10 nM, which was 500-1000 times lower than levels found in mammalian cultured cells (the expression is developmentally regulated; it was increased >100-fold at stages 25 or 26). Because the volume of one blastomere is ~0.5 μl, 50- and 25-nl injection would introduce 16.5 and 8.25 μM caldesmon, respectively. Although this would increase caldesmon concentration a 1000-fold higher than the level of endogenous caldesmon, the increased level is equivalent to the levels found in cultured cells. Also the increased caldesmon concentrations appear to just saturate F-actin in *Xenopus* eggs as judged from its F-actin content. *Xenopus* eggs were reported to contain ~100 μM actin, two-thirds of which (67 μM) appear to be either filamentous or oligomeric actin (Merriam and Clark, 1978). Because caldesmon saturates F-actin at a caldesmon-to-actin ratio of 1:6, >11 μM caldesmon would be required for saturation. This could be a reason why 50-nl injection gave more complete effects on *Xenopus* cell division.

Similar inhibition of cell division was observed with somatic cells such as CHO cells. CHO cells were treated with thymidine for 15 h for synchronization. After the release of thymidine block, cells were injected with either wild-type caldesmon, 7th mutant, or injection buffer alone. After 24-h incubation, effects on cell division were examined by counting cells with multinuclei. The fractions of cells with multinuclei were 6 ± 2% for buffer-injected cells, 13 ± 5% for cells injected with wild-type caldesmon, and 25 ± 5% for cells injected with mutant caldesmon. The extent of the inhibition is less than that found with *Xenopus* embryonic cell division. This may not be surprising, however, because adherent cells use additional mechanisms for the completion of cell division when one mechanism is impaired. For example, a myosin null mutant of *Dictyostelium* can divide by cytofission (myosin II-independent mechanism) when at-

Table 1. Inhibition of cell division of *Xenopus* embryos by 7th mutant

	Volume	Estimated final conc.*	No. of injection	Blockage	Delay	Normal
	nl	μM			%	
Buffer	50	0	42	0	2	98
Wild	50	16.5	64	5	29	66
Wild	25	8.25	41	2	37	61
7th	50	16.5	60	63	37	0
7th	25	8.25	22	14	82	5

* The needle concentration of caldesmon is 165 μM. The calculation is based on an estimate that the volume of one blastomere at the two-cell stage of *Xenopus* embryos is 0.5 μl.

tached on a substrate, but not when cultured in suspension (Manstein *et al.*, 1989).

Mutant Caldesmon Inhibits M-Phase Entry of CHO Cells

We next analyzed which stages of cell division 7th mutant affects. A likely stage is the G_2/M transition because 7th mutant would perturb the reorganization of the actin cytoskeleton during G_2/M transition, and may affect the entry into M-phase. To examine this possibility, we microinjected wild-type or mutant caldesmon into synchronized CHO cells to see effects on M-phase entry.

The synchronization of CHO cells was performed using thymidine block followed by nocodazole treatment as described in MATERIALS AND METHODS. Cells were fixed at the end of a 4-h nocodazole treatment and stained with 4,6-diamino-2-phenylindole (DAPI) to identify cells at mitosis by chromosome condensation. Two sets of microinjection experiments that differed in the timing of injection were performed. In the first set, we injected wild-type caldesmon or 7th mutant (5 mg/ml) before the thymidine treatment so that we were able to examine the effects of caldesmon 20–22 h after injection. In the second set, caldesmon was injected just before the nocodazole treatment, so that the effects of caldesmon were examined 4 h after injection. For these microinjection experiments, fluorescein isothiocyanate (FITC)-dextran was coinjected to identify injected cells.

The first set of experiments revealed that 7th mutant delayed the entry into M-phase. Figure 3, A–C, show a control experiment where buffer alone was injected. An FITC image (Figure 3A) demonstrated that many of the injected cells (about half in this particular field) exhibited rounded morphology characteristic of mitotic cells (indicated by arrowheads), whereas other injected cells (indicated by asterisks) were still in interphase. This is confirmed by an image of DAPI staining (Figure 3B) and by a phase-contrast image (Figure 3C). Uninjected cells present in the same field showed a similar population of mitotic cells, indicating that cells had recovered from the damage of microinjection during 20–22-h incubation.

Figure 3, D–F, show cells injected with wild-type caldesmon. Again, a similar population of injected cells (Figure 3D, indicated by arrowheads) entered mitosis as revealed by DAPI (Figure 3E) and phase-contrast (Figure 3F) images. In contrast, cells injected with 7th mutant (Figure 3G) were all flat (indicated by asterisks), indicating that they were not in a mitotic state. DAPI staining (Figure 3H) and phase-contrast (Figure 3I) images confirmed that none of them showed mitotic chromosome condensation. The quantitative results of three independent experiments are illustrated in Figure 4A. Injection of buffer and wild-type caldesmon resulted in the accumulation of mitotic cells to 38 ± 9 and 31 ± 7%, respectively. On the contrary, <5% of cells entered mitosis when injected with the mutant caldesmon.

The second set of experiments was designed to evaluate short-term (4-h incubation after injection) effects of caldesmon microinjection (Figure 4B). Again, 7th mutant was able to inhibit entry into M-phase. Approximately 10% of cells injected with 7th entered M-phase, whereas 26% of control cells injected with buffer alone became mitotic. There are, however, significant differences between the long-term (Figure 4A) and short-term (Figure 4B) effects. Both wild-type and mutant caldesmon caused similar delay in the M-phase entry when injected just before M-phase. In addition, the short-term effect of 7th mutant seemed to be less potent than the long-term effect: less than 5% of injected cells went into mitosis when cells were injected 20–22 h before, whereas 10% entered mitosis when injected 4 h before. It is also noticeable that cells may not be fully recovered from the damage of microinjection during the 4-h incubation because a lower population (26%) of cells injected with buffer alone went into M-phase, whereas as much as 40% of uninjected cells entered M-phase.

Inducible Expression of 7th Mutant Delays M-Phase Entry

We performed transfection experiments to further analyze the effects of caldesmon expression on cell cycle progression. We used the ecdysone-inducible expression system because our various attempts to isolate clones stably expressing full-length nonmuscle caldesmon all failed, suggesting that caldesmon expression may be toxic for cell proliferation. Five independent clones of CHO cells were isolated and monitored for the induction of wild-type and 7th caldesmon upon treatment with muristerone A. They all showed similar levels of caldesmon induction. After induction with 3 μM muristerone A for 24 h, cells accumulated up to ~0.08 to 0.1% of total protein for both wild-type and mutant caldesmon. Although this level is >8–10 times higher than the endogenous level (~0.01%) of caldesmon present in CHO cells, the increased level of caldesmon is roughly equivalent or at most 3 times higher than the levels of caldesmon present in well-spread fibroblasts such as NRK cells and REF52 cells. It also should be noted that a certain fraction of cells kept losing the ability to induce exogenous expression of caldesmon during propagation: Approximately 70% of cells showed induced expression of caldesmon.

We examined effects of caldesmon induction on M-phase entry. After addition of muristerone A, the cell cycle of transfected CHO cells was synchronized by the sequential treatment with thymidine and nocodazole in the same way as described before. After 3-h incubation with nocodazole, cells were simultaneously stained with the anti-myc antibody and DAPI, to detect cells exogenously expressing wild-type or mutant caldesmon, and to determine whether cells were in mitosis, respectively.

As Figure 5 shows, cells expressing mutant caldesmon have a much lower population of mitotic cells: only 5–8% of cells expressing mutant caldesmon became mitotic, the value of which was greatly lower than that (~30%) shown by control mock-transfected cells. On the other hand, the induction of wild-type caldesmon was less effective in delaying M-phase entry: Approximately 17–23% of cells expressing wild-type caldesmon were found in mitosis. These results again indicate that expression of mutant caldesmon effectively delays M-phase entry, the result of which is consistent with the microinjection experiments.

Stabilization of Microfilaments by 7th Mutant

We then examined whether the induced expression of wild-type caldesmon or 7th mutant alters actin assembly during mitosis. Cells at the end of the 3-h nocodazole treatment were stained with rhodamine phalloidin to examine the organization of F-actin. Simultaneous staining with the myc

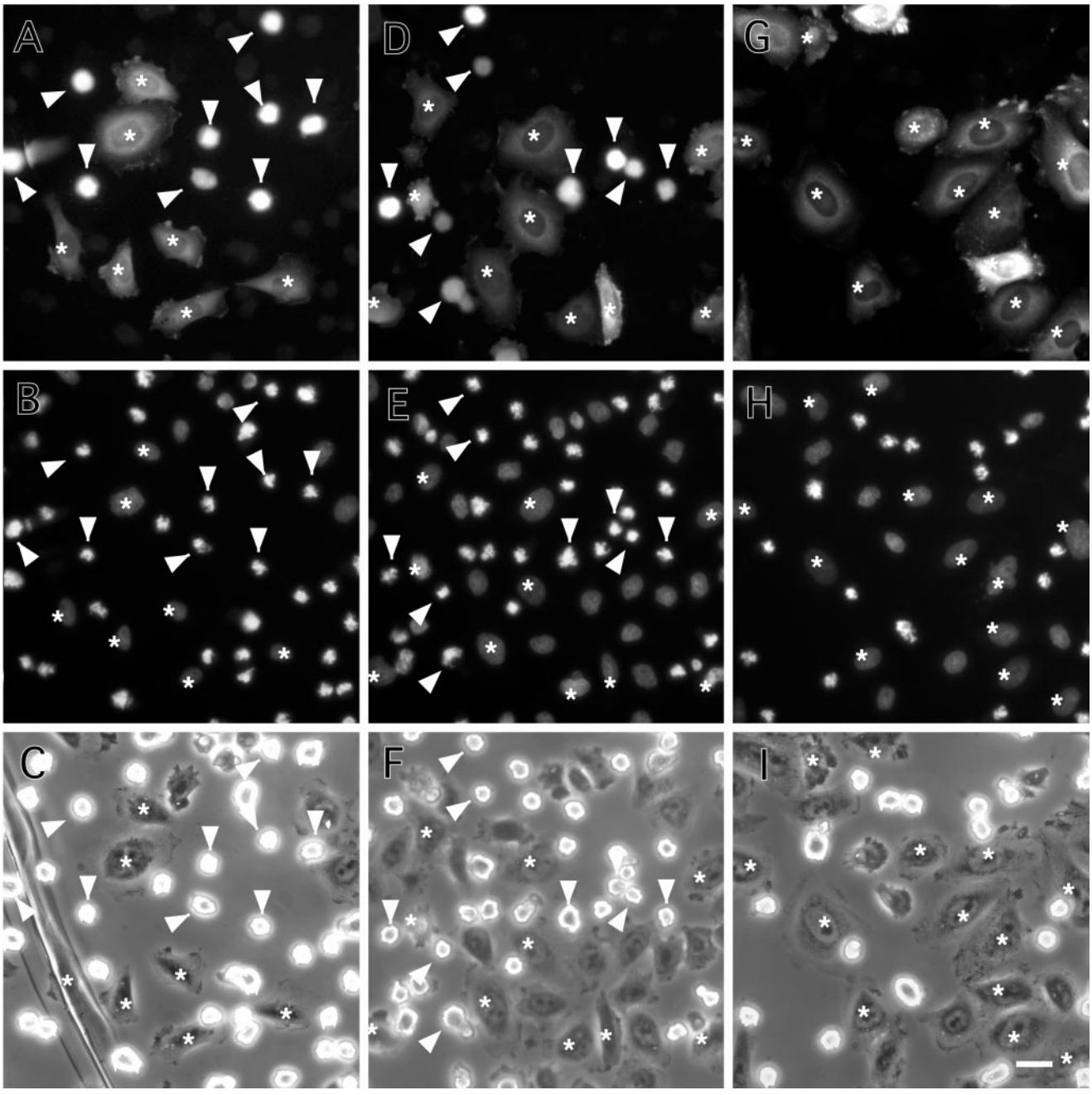

Figure 3. Delay of M-phase entry by microinjection of 7th mutant. CHO cells were microinjected with buffer alone (A–C), wild-type caldesmon (D–F), or 7th mutant caldesmon (G–I). FITC-dextran was coinjected to identify injected cells (A, D, and G). Cells were then synchronized for cell division by thymidine treatment followed by nocodazole treatment as described in MATERIALS AND METHODS. After 4 h of nocodazole treatment, cells were fixed and stained with DAPI to examine chromosome condensation (B, E, and H). (C, F, and I) Corresponding phase-contrast images of the same fields. Arrowheads and asterisks indicate mitotic and nonmitotic cells, respectively. Note that none of cells injected with 7th mutant caldesmon were in mitosis as judged by their flat morphology (G), and by DAPI staining (H). On the contrary, about half of cells injected with either buffer alone (A–C) or wild-type caldesmon (D–F) went into mitosis as judged by their morphology (A and D) and by chromosome condensation (B and E). Bar, 25 μm.

antibody and DAPI was performed to examine exogenous expression of caldesmon and chromosome condensation, respectively.

Figure 6 shows representative deconvolution images of mock-transfected (Figure 6, A–C), wild-type caldesmon-expressing (Figure 6, D–I), and 7th mutant-expressing (Figure

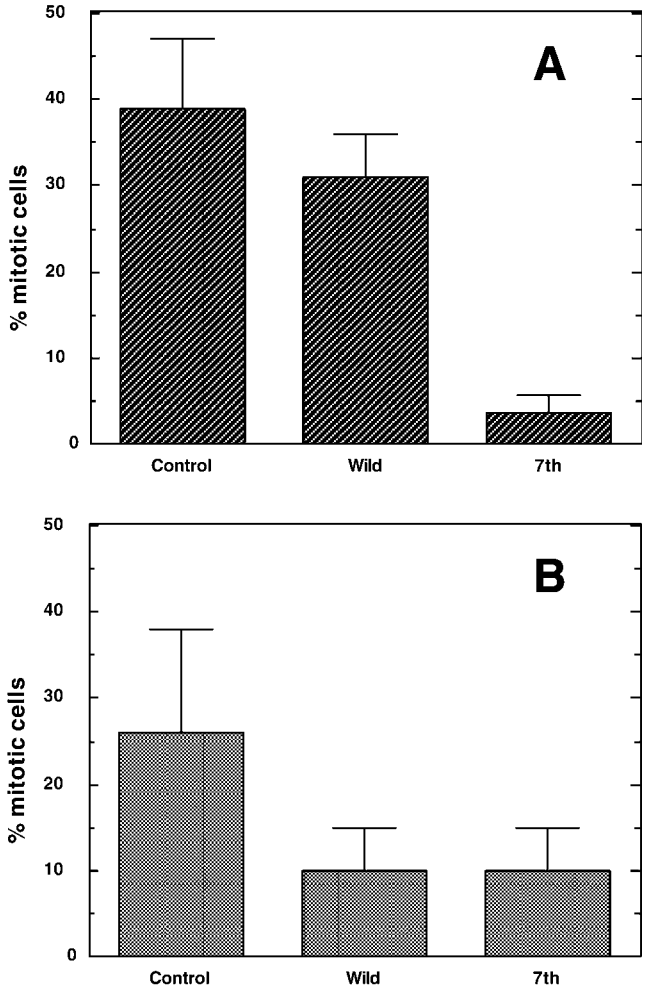

Figure 4. Effects of caldesmon injection on the entry into M-phase. (A) Long-term effects of caldesmon injection on M-phase entry. Microinjection was performed before thymidine treatment as described in Figure 3. About 100 cells were injected. Number of cells in mitosis was counted and expressed as percentage of mitotic cells per total number of injected cells. Note that only 7th delayed M-phase entry. Three independent experiments were performed. (B) Short-term effects of caldesmon injection on M-phase entry. Microinjection was performed before nocodazole treatment. Note that both wild-type and mutant caldesmon delayed M-phase entry. Three independent experiments were performed.

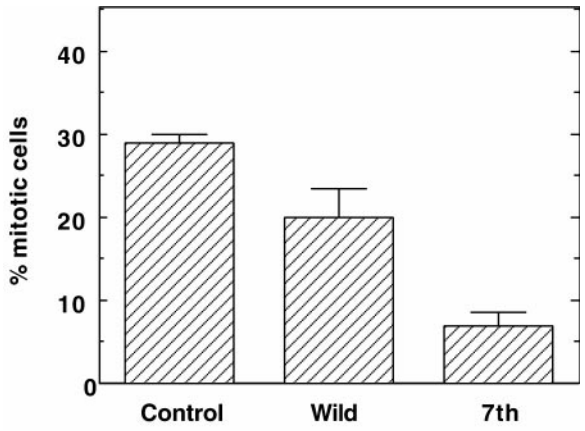

Figure 5. Delay of M-phase entry by inducible expression of 7th mutant caldesmon. Expression of caldesmon was induced by the addition of muristerone A before thymidine treatment. Cells were fixed after 3 h of nocodazole treatment, and double-labeled with myc antibody and DAPI. Cells showing chromosome condensation were counted as mitotic cells. Control indicates mock-transfected cells treated in the same way. About 100–200 cells were examined for each experiment and three independent experiments were performed.

6, J–R), rounded cells either in mitosis or near mitosis. In the case of mock transfection (Figure 6, A–C), ~70% of rounded cells (n = 236) were in mitosis as indicated by chromosome condensation. Phalloidin staining of these mitotic cells showed weak cortical staining. No microfilament bundles were observed with these cells (Figure 6B).

In the case of inducible expression of wild-type caldesmon (Figure 6, D–I), only half (44%) of rounded cells was found to be in mitosis by DAPI staining (n = 282). Mitotic rounded cells expressing wild-type caldesmon tended to show slightly higher cortical F-actin staining (Figure 6E) than did the mock-transfected rounded cells (Figure 6B). The localization of wild-type caldesmon in such cells was, however, diffuse (Figure 6D), suggesting that caldesmon was mostly dissociated from microfilaments. The diffused localization of myc-tagged exogenous caldesmon is similar to the localization of endogenous caldesmon during mitosis as previously reported (Hosoya *et al.*, 1993). In contrast, >90% of nonmitotic rounded cells expressing wild-type caldesmon (Figure 6, G–I) exhibited filamentous actin bundles stained with both the anti-myc antibody (Figure 6G) and phalloidin (Figure 6H). Frequently, these cells showed stronger staining of actin cortex (indicated by arrow) than mock-transfected rounded cells. This observation suggests that phosphorylation of wild-type caldesmon by cdc2 kinase may be incomplete in these cells, thereby inhibiting microfilament disassembly in prophase.

As described (Figure 5), the induction of 7th mutant inhibited the entry into M-phase (only 5–8% of 7th-expressing cells were rounded mitotic cells versus ~20% of wild caldesmon-expressing cells). Although the number of 7th-expressing rounded cells was small, we were able to examine 136 of such rounded cells and examined what effects 7th has on actin organization of these cells. As Figure 6, J–R, shows, these rounded cells showed stabilized microfilament assembly. About half (55%) of rounded cells expressing 7th mutant was found to be mitotic, the percentage of which was similar to that (44%) found with the expression of wild-type caldesmon. Unlike the expression of wild-type caldesmon, however, rounded mitotic cells expressing 7th mutant (arrow in Figure 6, J–L) frequently retained actin filament bundles inside cells that were stained by phalloidin (Figure 6K). Although the background of myc staining was high, these actin bundles appeared to be labeled with the myc antibody (Figure 6J), indicating that 7th mutant was not dissociated from microfilaments during mitosis. Quantification revealed that more than 65% of 7th-expressing mitotic rounded cells retained microfilament bundles. In contrast, <20% of mitotic cells expressing wild-type caldesmon showed filamentous

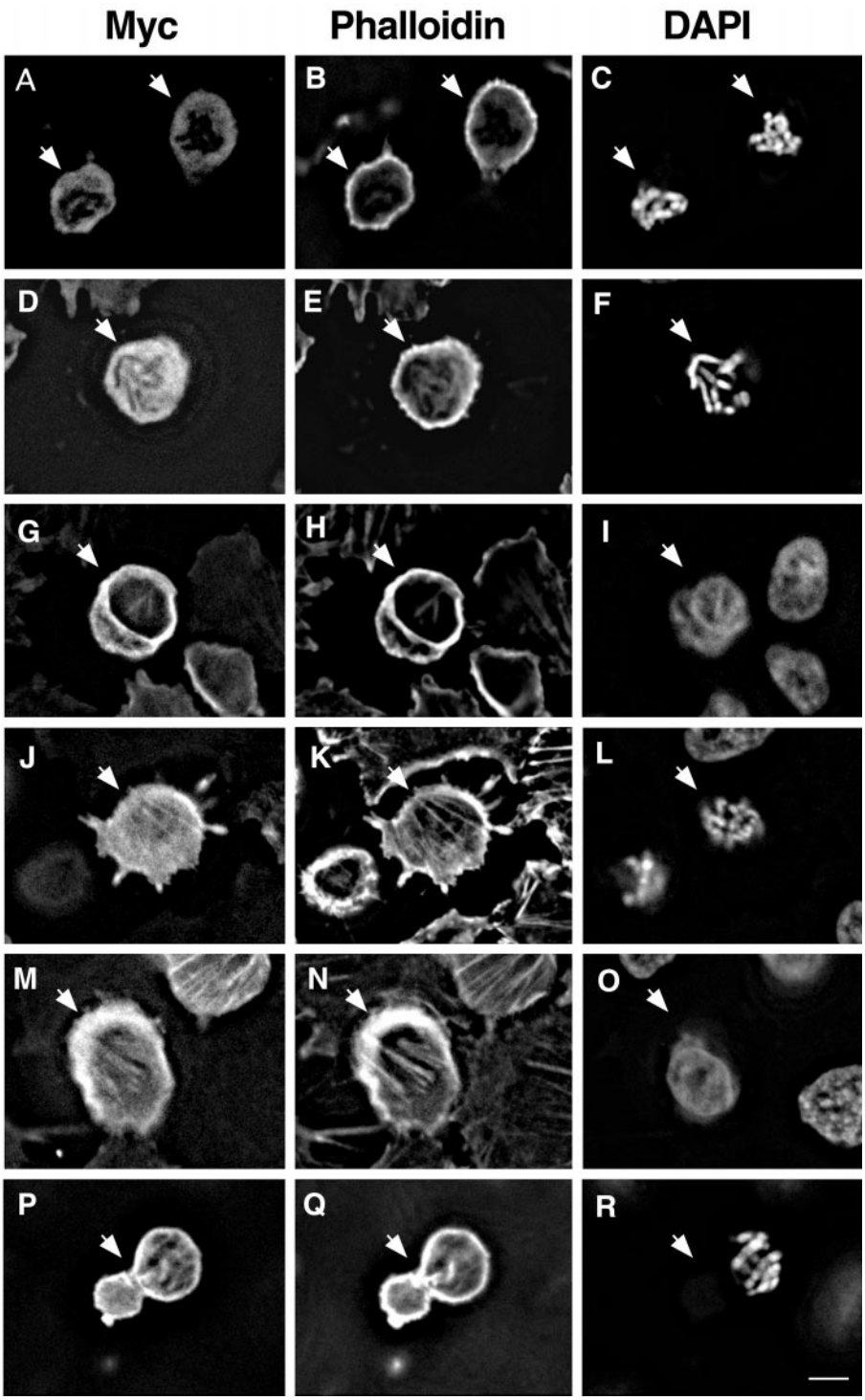

Figure 6. Inducible expression of 7th mutant caldesmon stabilizes microfilaments during mitosis. Wild-type or mutant caldesmon was inducibly expressed before thymidine treatment and cells were fixed after 3 h of nocodazole treatment. Rounded cells were examined by staining with myc antibody (A, D, G, J, M, and P), rhodamine phalloidin (B, E, H, K, N, and Q), and DAPI (C, F, I, L, O, and R). Images were deconvolved using VayTek Microtome software. (A–C) Mock-transfection. Arrows indicate mitotic rounded cells. (D–I) Rounded cells expressing wild-type caldesmon (indicated by arrow). A mitotic rounded cell expressing wild-type caldesmon (D–F) showed a slightly higher cortex staining with phalloidin (E), whereas myc-staining (D) was diffuse. Nonmitotic rounded cells (arrow in G–I), on the other hand, exhibited actin bundles inside the cell or cortex that were stained both with myc antibody (G) and phalloidin (H). (J–R) Rounded cells expressing 7th mutant caldesmon. A mitotic cell (arrow in J–L) retained actin bundles that were stained both with myc antibody (J) and phalloidin (K). A nonmitotic rounded cell (indicated by arrow in M–O) showed stress fibers stained with both myc antibody and phalloidin. (P–R) Dumbbell-shaped mitotic cells expressing 7th mutant. Bar, 10 μm.

actin bundles. Nonmitotic rounded cells expressing 7th mutant (arrow in Figure 6, M–O) also showed stabilized microfilaments: 90% of them maintained stress fiber-like structures that were stained with both the myc-antibody (Figure 6M) and phalloidin (Figure 6N).

Expression of 7th mutant generated a large number (30% of 7th-expressing mitotic cells) of dumbbell-shaped mitotic cells (Figure 6, P–R). These cells had filamentous actin bundles that were stained both with the myc antibody (Figure 6P) and phalloidin (Figure 6Q). The cortex also showed

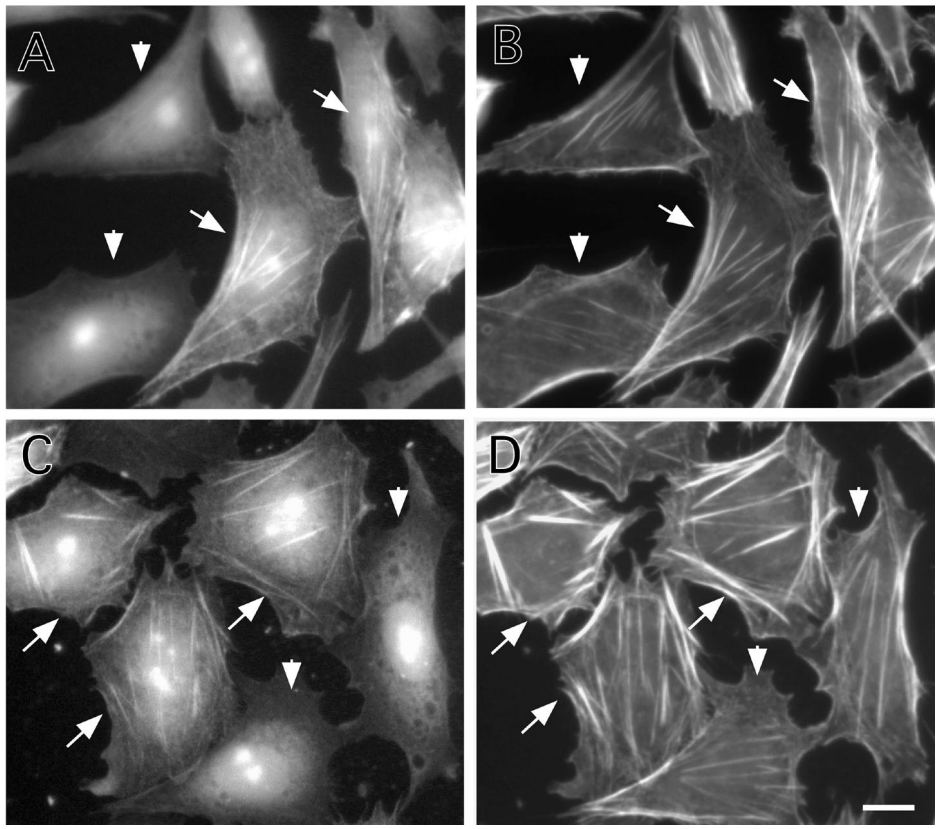

Figure 7. Stabilization of microfilaments by expression of 7th mutant caldesmon. Wild-type (A and B) or 7th mutant (C and D) caldesmon was inducibly expressed for 24 h by using the ecdysone expression system. Cells were stained with the myc antibody to detect exogenously expressed wild-type (A) or 7th mutant (C) caldesmon, and counterstained with rhodamine phalloidin to reveal microfilaments (B and D). Arrows indicate cells inducibly expressing caldesmon, whereas arrowheads show nonexpressing cells. Note that stress fibers of cells expressing 7th mutant caldesmon are thicker than those of nonexpressing cells (D). Bar, 10 μm.

strong staining with phalloidin and the myc antibody. Interestingly, one lobe of dumbbell-shaped cells was always larger than the other, and the larger lobe contained condensed chromosomes in most cases (Figure 6R). These deformed mitotic cells appeared to be characteristic of 7th-expressing mitotic CHO cells: only 3% of wild-type caldesmon-expressing mitotic cells and virtually none of mock-transfected mitotic cells showed such morphology after 3 h of nocodazole treatment. The retained actin bundles and strong cortex staining again indicate that 7th mutant stabilizes microfilaments during mitosis. The dumbbell-shaped morphology suggests that cells may undergo premature cytokinesis.

Effects of caldesmon expression on the actin cytoskeleton of interphase cells also were examined. Figure 7 shows CHO cells that were induced to express either wild-type caldesmon (Figure 7, A and B) or 7th (Figure 7, C and D) by addition of muristerone A for 24 h. Cells were stained by the myc antibody to identify cells exogenously expressing caldesmon (Figure 7, A and C), and by rhodamine phalloidin to reveal F-actin organization of such cells (Figure 7, B and D). The micrographs were taken to include both caldesmon-expressing (indicated by arrow) and -nonexpressing (indicated by arrowhead) cells so that the organization of actin in these two types of cells could be compared. The expression of 7th mutant induced assembly of thick stress fibers in the center of most cells (arrow in Figure 7, C and D). Although wild-type caldesmon seemed to have similar effects in some cells, it was less effective than 7th mutant.

Myc and phalloidin staining intensities of mock-transfected, wild-type caldesmon-expressing, and 7th mutant-expressing cells were measured to quantitatively address the effects of caldesmon expression on F-actin stability (Figure 8). A majority (85%) of cells expressing 7th mutant exhibits phalloidin staining higher than that shown by mock-transfected cells (above a dotted horizontal line in Figure 8). On the other hand, 65% of cells expressing wild-type caldesmon show phalloidin staining similar to that of mock-transfected cells. We compared the average F-actin intensities of wild-type caldesmon-expressing and 7th mutant-expressing cells with the average intensity of mock-transfected cells. The average values are increased by 2.3 $\pm$ 0.5-fold for 7th mutant-expressing cells and 1.6 $\pm$ 0.4-fold for wild-type caldesmon-expressing cells. These observations support the notion that caldesmon plays a role in stabilizing microfilaments, and suggest that caldesmon phosphorylation also may regulate microfilament stability during interphase. It is also worthy of note that the induced levels of exogenous caldesmon are not unphysiologically high. The myc-staining of wild-type and 7th caldesmon (Figure 7, A and C) exhibited localization on stress fibers, as well as at cell periphery, but did not show a high background of diffuse cytoplasmic staining or unusual structures of microfilaments. These staining patterns are similar to those of endogenous caldesmon previously reported by others and us (Bretscher and Lynch, 1985; Dingus *et al.*, 1986; Yamashiro-Matsumura *et al.*, 1988; Yamashiro-Matsumura and Matsumura, 1988).

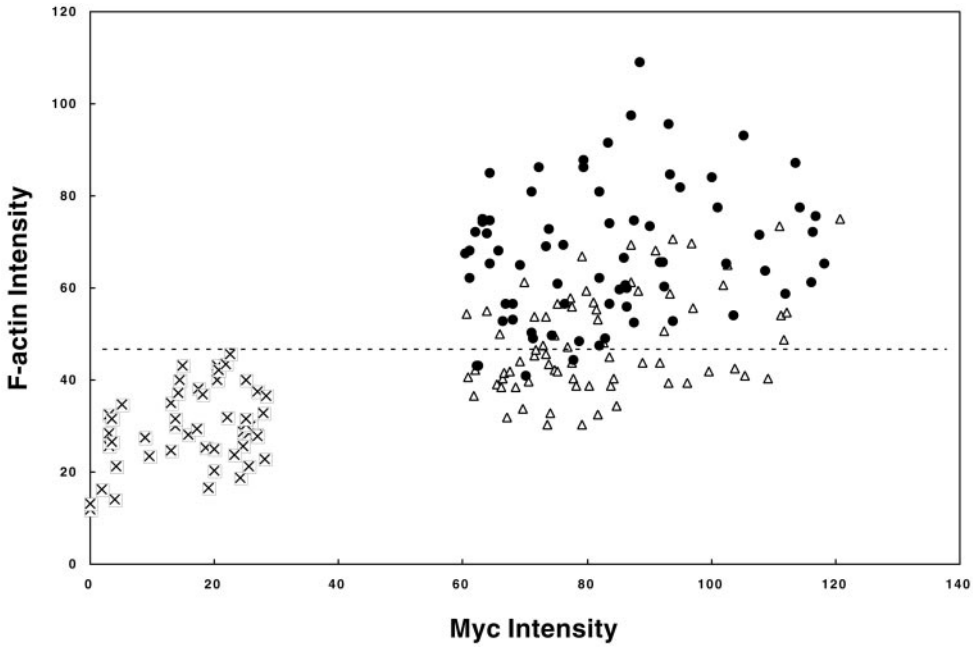

Figure 8. Quantitative fluorescence measurement of myc and phalloidin staining intensities of mock-transfected (☒), wild-type caldesmon-expressing (△), and 7th mutant caldesmon-expressing (●) cells. Mean fluorescence intensities (arbitrary unit) of cells expressing caldesmon were quantitated with NIH image software. The dashed line in the figure shows a maximum fluorescent intensity of phalloidin staining of mock-transfected cells, intensities above which are judged to have higher F-actin staining than control.

7th Mutant Caldesmon Does Not Inhibit Cyclin B/cdc2 Kinase

It is possible that 7th mutant caldesmon could inhibit cyclin B/cdc2 kinase, thereby inhibiting M-phase entry. We have thus examined effects of wild-type and 7th mutant caldesmon on the histone H1 kinase activity of cyclin B/cdc2. Cyclin B1/cdc2 kinase were immunoprecipitated from mitotically arrested HeLa cells. Approximately 5 times molar excess amount of wild-type or 7th mutant caldesmon was added over histone H1, so that inhibition by caldesmon, if any, could be detected. As Figure 9 shows, however, 7th caldesmon has no inhibitory effects on cyclin B1/cdc2 histone H1 kinase activity. Wild-type caldesmon shows slight inhibition (5–10%), which is perhaps due to the competitive inhibition by wild-type caldesmon. We also examined effects of caldesmon and 7th mutant using recombinant cdc2 kinase. Again neither wild-type nor 7th caldesmon inhibited the histone H1 kinase activity (our unpublished results). These results suggest that the inhibitory effects of 7th mutant on cell division are not due to direct inhibition of cyclin B/cdc2 activity.

DISCUSSION

This work has demonstrated two major effects of the phosphorylation mutant of caldesmon: 1) 7th mutant delays the entry into M-phase and inhibits cytokinesis; and 2) the mutant stabilizes the actin cytoskeleton during G_2/M transition, thus inhibiting cell rounding. The latter effect has been predicted previously (Matsumura and Yamashiro, 1993) because mutant caldesmon would stay bound to microfilaments during mitosis and because stabilization of microfilaments appears to be caldesmon's function both in vitro and in vivo (reviewed by Matsumura and Yamashiro, 1993; Huber, 1997).

How could 7th mutant delay M-phase entry? Most normal adherent cells disassemble stress fibers and become rounded during G_2/M transition. These morphological alterations appear to be physiologically significant in two ways. First, the disassembly of stress fibers may be required for cells to prepare for cytokinesis because the assembly of contractile rings would be regulated in a way very different from that of stress fibers. It is thus possible that cells may have a mechanism to delay M-phase entry when the disassembly of

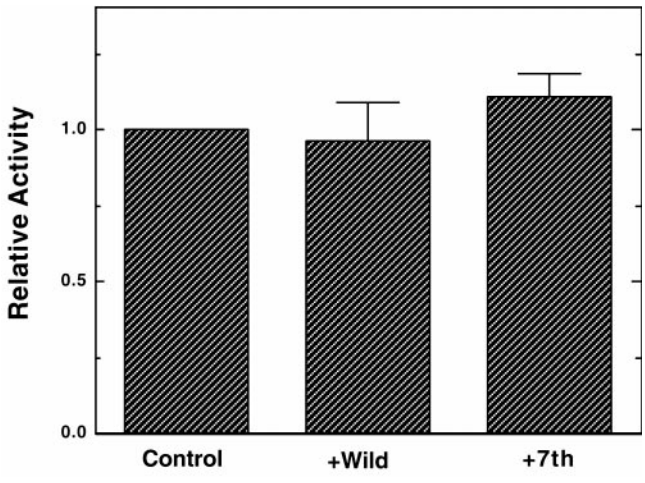

Figure 9. No effects of 7th mutant caldesmon on cyclin B/cdc2 kinase activities. Histone H1 kinase activities of cyclin B1/cdc2 immune-complex were examined in the absence (control) or presence of wild-type or 7th mutant. The activities were expressed relative to the control. Four independent experiments were performed for each immune-complex.

stress fibers is inhibited. Second, cell rounding may be important to control signal transduction for cell proliferation. Most normal adherent cultured cells show a cycle of cell rounding during prophase and cell spreading after cell division. Because cell rounding during prophase results in the loss of cell adhesions, mitotic cell rounding is most likely to turn "off" adhesion-mediated signal transduction machinery. This off state should be essential for the signal transduction machinery to be turned "on" later during postmitotic cell spreading, which is known to be critical for cell cycle progression. It is thus possible that normal adherent cells may have a mechanism that ensures the inactivation of adhesion-meditated signaling by cell rounding during prophase. In either case, the inhibition of cell rounding by 7th mutant may result in delay in M-phase entry. We are in the process of investigating these possibilities.

The effects of caldesmon on M-phase entry depend on the timing of microinjection. Wild-type caldesmon injected before thymidine treatment produced little effect (Figure 4A). However, both wild-type and mutant caldesmon, when injected just before M-phase, caused similar delays in M-phase entry (Figure 4B), though the magnitude of the effects was much less than that shown by the mutant injection before thymidine treatment. The exact reason for this difference is not clear at this time, however, it might be explained in the following way. Wild-type caldesmon is a very good substrate of cdc2 kinase because it can be phosphorylated at a ratio of up to 7 mol/mol. Cdc2 kinase may not be able to phosphorylate all wild-type caldesmon completely if its concentration is suddenly increased by microinjection just before M-phase.

The blockage of cell division also may be due to caldesmon's effects in stabilizing microfilaments. Such stabilization would alter the interactions between actin and other actin-binding proteins, altering the dynamics of actin assembly during cytokinesis. For example, we previously demonstrated that caldesmon together with tropomyosin blocks actin-severing and -capping activities of gelsolin (Ishikawa *et al.*, 1989a,b). Likewise, we have recently found that the same protein combination inhibits cofilin's actin binding as well as its actin depolymerization activity (our unpublished results). Cofilin activities have to be precisely regulated during cell division because Abe *et al.* (1996) have reported that injection with either constitutively active cofilin or function-inhibiting antibody against cofilin blocks cell division of *Xenopus* embryos. It is thus possible that 7th mutant caldesmon may interfere with cofilin/actin interactions. The dumbbell-shaped morphology observed with cells expressing 7th mutant may be caused by the changes in the actin dynamics and/or the regulation of contractile activity.

We observed that the expression of caldesmon results in the induction of thicker stress fibers during interphase and the mutant is again more effective (Figure 7). This effect of microfilament stabilization is consistent with the previous reports by others and by us (reviewed by Matsumura and Yamashiro, 1993; Huber, 1997) but is in contrast to the recent report that caldesmon overexpression inhibits stress fiber formation (Helfman *et al.*, 1999). The reason for this discrepancy is not clear at present. One reason could be the differences in cell lines and/or ectopic expression systems. The discrepancy also may be due to the difference in the expression level of caldesmon: the ecdysone-inducible system used in this study appears to express a lower level of caldesmon than transient overexpression used in their study. In our case, exogenous caldesmon is mostly associated with microfilaments and little free caldesmon was observed in the cytoplasm. Indeed, we observed disorganization of microfilaments when caldesmon expression became very high (our unpublished results).

7th mutant is more effective in stabilizing microfilaments during interphase than is wild-type caldesmon. This effect may be explained by the fact that caldesmon is phosphorylated by mitogen-activated protein kinase (MAPK). MAPK was reported to be activated in G_0/G_1 and/or G_1 through S phases of the cell cycle (Tamemoto *et al.*, 1992; Watson *et al.*, 1993). This activity is likely to correspond to a caldesmon kinase activity observed in G_0/G_1 transition (Watson *et al.*, 1993). Indeed, a recent report has shown a rapid increase in MAPK-dependent phosphorylation of caldesmon upon serum stimulation of cultured smooth muscle cells (D'Angelo *et al.*, 1999). Because the sites of MAPK phosphorylation are a subset of the cdc2 kinase sites (Childs *et al.*, 1992; Adam and Hathaway, 1993; Redwood *et al.*, 1993), such phosphorylation would inhibit, to a certain extent, the activities of wild-type caldesmon, however the mutant caldesmon would not be affected.

Our results suggest that there may be a mechanism by which the caldesmon-mediated regulation of microfilament organization affects cell cycle progression at M-phase. The critical role of caldesmon in cell division is reinforced by the observation that it is difficult, though may not be impossible, to isolate transfectants stably expressing full-length caldesmon (our unpublished results; Surgucheva and Bryan, 1995). Our results appear to explain, at least in part, why caldesmon expression is suppressed upon cell transformation (Owada *et al.*, 1984; Novy *et al.*, 1991; Yamashiro *et al.*, 1994), and why stress fibers are disorganized in many transformed cells.

ACKNOWLEDGMENTS

We thank Dr. F. Deis (Rutgers University) for critical reading of this manuscript. This work was supported by a grant CA-42742 to F.M. and S.Y. F.M. is a member of the Cancer Institute of New Jersey.

REFERENCES

Abe, H., Obinata, T., Minamide, L.S., and Bamburg, J.R. (1996). *Xenopus laevis* actin-depolymerizing factor/cofilin: a phosphorylation-regulated protein essential for development. J. Cell Biol. *132*, 871–885.

Adam, L.P., and Hathaway, D.R. (1993). Identification of mitogen-activated protein kinase phosphorylation sequences in mammalian h-Caldesmon. FEBS Lett. *322*, 56–60.

Bradford, M. (1976). A rapid and sensitive method for the quantitation of microgram quantities of protein utilizing the principle of protein-dye binding. Anal. Biochem. *72*, 248–254.

Bretscher, A. (1984). Smooth muscle caldesmon. Rapid purification and F-actin crosslinking properties. J. Biol. Chem. *259*, 12873–12880.

Bretscher, A., and Lynch, W. (1985). Identification and localization of immunoreactive forms of caldesmon in smooth and nonmuscle cells: a comparison with the distributions of tropomyosin and alpha-actinin. J. Cell Biol. *100*, 1656–1663.

Burton, D.J., and Marston, S.B. (1999). Control of shortening speed in single guinea-pig *Taenia coli* smooth muscle cells by Ca^{2+}, phosphorylation and caldesmon. Pflügers Arch. *437*, 267–275.

Castellino, F., Ono, S., Matsumura, F., and Luini, A. (1995). Essential role of caldesmon in the actin filament reorganization induced by glucocorticoids. J. Cell Biol. *131*, 1223–1230.

Childs, T.J., Watson, M.H., Sanghera, J.S., Campbell, D.L., Pelech, S.L., and Mak, A.S. (1992). Phosphorylation of smooth muscle caldesmon by mitogen-activated protein (MAP) kinase and expression of MAP kinase in differentiated smooth muscle cells. J. Biol. Chem. *267*, 22853–22859.

D'Angelo, G., Graceffa, P., Wang, C.A., Wrangle, J., and Adam, L.P. (1999). Mammal-specific, ERK-dependent, caldesmon phosphorylation in smooth muscle. Quantitation using novel anti-phosphopeptide antibodies J. Biol. Chem. *274*, 30115–30121.

Dingus, J., Hwo, S., and Bryan, J. (1986). Identification by monoclonal antibodies and characterization of human platelet caldesmon. J Cell Biol. *102*, 1748–1757.

Earley, J.J., Su, X., and Moreland, R.S. (1998). Caldesmon inhibits active crossbridges in unstimulated vascular smooth muscle: an antisense oligodeoxynucleotide approach. Circ. Res. *83*, 661–667.

Helfman, D.M., Levy, E.T., Berthier, C., Shtutman, M., Riveline, D., Grosheva, I., Lachish-Zalait, A., Elbaum, M., and Bershadsky, A.D. (1999). Caldesmon inhibits nonmuscle cell contractility and interferes with the formation of focal adhesions. Mol. Biol. Cell *10*, 3097–3112.

Hosoya, N., Hosoya, H., Yamashiro, S., Mohri, H., and Matsumura, F. (1993). Localization of caldesmon and its dephosphorylation during cell division. J. Cell Biol. *121*, 1075–1082.

Huber, P.A. (1997). Caldesmon. Int. J. Biochem. Cell Biol. *29*, 1047–1051.

Ishikawa, R., Yamashiro, S., and Matsumura, F. (1989a). Annealing of gelsolin-severed actin fragments by tropomyosin in the presence of Ca^{2+}. Potentiation of the annealing process by caldesmon. J. Biol. Chem. *264*, 16764–16770.

Ishikawa, R., Yamashiro, S., and Matsumura, F. (1989b). Differential modulation of actin-severing activity of gelsolin by multiple isoforms of cultured rat cell tropomyosin. Potentiation of protective ability of tropomyosins by 83-kDa nonmuscle caldesmon. J. Biol. Chem. *264*, 7490–7497.

Katsuyama, H., Wang, C.L., and Morgan, K.G. (1992). Regulation of vascular smooth muscle tone by caldesmon. J. Biol. Chem. *267*, 14555–14558.

Lamb, N.J., Fernandez, A., Mezgueldi, M., Labbe, J.P., Kassab, R., and Fattoum, A. (1996). Disruption of the actin cytoskeleton in living nonmuscle cells by microinjection of antibodies to domain-3 of caldesmon. Eur. J. Cell Biol. *69*, 36–44.

Mak, A.S., Carpenter, M., Smillie, L.B., and Wang, J.H. (1991). Phosphorylation of caldesmon by p34cdc2 kinase. Identification of phosphorylation sites. J. Biol. Chem. *266*, 19971–19975.

Manstein, D.J., Titus, M.A., De Lozanne, A., and Spudich, J.A. (1989). Gene replacement in *Dictyostelium*: generation of myosin null mutants. EMBO J. *8*, 923–932.

Matsumura, F., and Yamashiro, S. (1993). Caldesmon. Curr. Opin. Cell Biol. *5*, 70–76.

Merriam, R.W., and Clark, T.G. (1978). Actin in *Xenopus* oocytes. II. Intracellular distribution and polymerizability. J. Cell Biol. *77*, 439–447.

Novy, R.E., Lin, J.L., and Lin, J.J. (1991). Characterization of cDNA clones encoding a human fibroblast caldesmon isoform and analysis of caldesmon expression in normal and transformed cells. J. Biol. Chem. *266*, 16917–16924.

Owada, M.K., Hakura, A., Iida, K., Yahara, I., Sobue, K., and Kakiuchi, S. (1984). Occurrence of caldesmon (a calmodulin-binding protein) in cultured cells: comparison of normal and transformed cells. Proc. Natl. Acad. Sci. USA *81*, 3133–3137.

Pfitzer, G., Zeugner, C., Troschka, M., and Chalovich, J.M. (1993). Caldesmon and a 20-kDa actin-binding fragment of caldesmon inhibit tension development in skinned gizzard muscle fiber bundles. Proc. Natl. Acad. Sci. USA *90*, 5904–5908.

Redwood, C.S., Marston, S.B., and Gusev, N.B. (1993). The functional effects of mutations Thr673→Asp and Ser702→Asp at the Pro-directed kinase phosphorylation sites in the C-terminus of chicken gizzard caldesmon. FEBS Lett. *327*, 85–89.

Sobue, K., Muramoto, Y., Fujita, M., and Kakiuchi, S. (1981). Purification of a calmodulin-binding protein from chicken gizzard that interacts with F-actin. Proc. Natl. Acad. Sci. USA *78*, 5652–5655.

Surgucheva, I., and Bryan, J. (1995). Over-expression of smooth muscle caldesmon in mouse fibroblasts. Cell. Motil. Cytoskeleton *32*, 233–243.

Tamemoto, H., Kadowaki, T., Tobe, K., Ueki, K., Izumi, T., Chatani, Y., Kohno, M., Kasuga, M., Yazaki, Y., and Akanuma, Y. (1992). Biphasic activation of two mitogen-activated protein kinases during the cell cycle in mammalian cells. J. Biol. Chem. *267*, 20293–20297.

Warren, K.S., Lin, J.L., Wamboldt, D.D., and Lin, J.J. (1994). Overexpression of human fibroblast caldesmon fragment containing actin-, Ca^{++}/calmodulin-, and tropomyosin-binding domains stabilizes endogenous tropomyosin and microfilaments. J. Cell Biol. *125*, 359–368.

Watson, M.H., Venance, S.L., Pang, S.C., and Mak, A.S. (1993). Smooth muscle cell proliferation. Expression and kinase activities of p34cdc2 and mitogen-activated protein kinase homologues. Circ. Res. *73*, 109–117.

Yamakita, Y., Yamashiro, S., and Matsumura, F. (1990). Microinjection of nonmuscle and smooth muscle caldesmon into fibroblasts and muscle cells. J. Cell Biol. *111*, 2487–2498.

Yamakita, Y., Yamashiro, S., and Matsumura, F. (1992). Characterization of mitotically phosphorylated caldesmon. J. Biol. Chem. *267*, 12022–12029.

Yamashiro, S., Yamakita, Y., Hosoya, H., and Matsumura, F. (1991). Phosphorylation of non-muscle caldesmon by p34cdc2 kinase during mitosis. Nature *349*, 169–172.

Yamashiro, S., Yamakita, Y., Ishikawa, R., and Matsumura, F. (1990). Mitosis-specific phosphorylation causes 83K non-muscle caldesmon to dissociate from microfilaments. Nature *344*, 675–678.

Yamashiro, S., Yamakita, Y., Ono, S., and Matsumura, F. (1998). Fascin, an actin-bundling protein, induces membrane protrusions and increases cell motility of epithelial cells. Mol. Biol. Cell. *9*, 993–1006.

Yamashiro, S., Yamakita, Y., Yoshida, K., Takiguchi, K., and Matsumura, F. (1995). Characterization of the COOH terminus of nonmuscle caldesmon mutants lacking mitosis-specific phosphorylation sites. J. Biol. Chem. *270*, 4023–4030.

Yamashiro, S., Yoshida, K., Yamakita, Y., and Matsumura, F. (1994). Caldesmon: possible functions in microfilament reorganization during mitosis and cell transformation. In: International Conference on the Biophysics, Biochemistry, and Cell Biology of Actin, ed. J.E. Estes, and P.J. Higgins. Troy, New York: Plenum Publishing, 113–122.

Yamashiro-Matsumura, S., Ishikawa, R., and Matsumura, F. (1988). Purification and characterization of 83kDa nonmuscle caldesmon from cultured rat cells: changes in its expression upon L6 myogenesis. Protoplasma *2* (suppl), 9–21.

Yamashiro-Matsumura, S., and Matsumura, F. (1988). Characterization of 83-kilodalton nonmuscle caldesmon from cultured rat cells: stimulation of actin binding of nonmuscle tropomyosin and periodic localization along microfilaments like tropomyosin. J. Cell. Biol. *106*, 1973–1983.